Stem Cell Research 53 (2021) 102263

Contents lists available at ScienceDirect

Stem Cell Research

journal homepage: www.elsevier.com/locate/scr

Lab resource: Stem Cell Line

Generation and cardiac differentiation of an induced pluripotent stem cell line from a patient with arrhythmia-induced cardiomyopathy

Sabine Rebs [a,1], Jakob Beier [a,1], Loukas Argyriou [b], Tillmann Schill [c], Gerd Hasenfuss [a], Dirk Vollmann [d], Samuel Sossalla [a,e,2], Katrin Streckfuss-Bömeke [a,2,*]

[a] Clinic for Cardiology & Pneumology, University Medical Center Goettingen, and DZHK (German Centre for Cardiovascular Research), partner site Goettingen, Germany
[b] Institute of Human Genetics, University Medical Center Goettingen, and DZHK (German Centre for Cardiovascular Research), partner site Goettingen, Germany
[c] Department of Dermatology, Venereology and Allergology, University Medical Center Goettingen, Goettingen, Germany
[d] Herz- & Gefäßzentrum Goettingen, Goettingen, Germany
[e] Clinic and Polyclinic for Internal Medicine II, University Medical Center Regensburg, Regensburg, Germany

A B S T R A C T

Arrhythmia-induced cardiomyopathy (AIC) is characterized by left-ventricular systolic dysfunction caused by persistent arrhythmia. To date, genetic or pathological drivers causing AIC remain unknown. Here, we generated induced pluripotent stem cells (iPSCs) from an AIC patient. The AIC-iPSCs exhibited full pluripotency and differentiation characteristics and maintained a normal karyotype after reprogramming. The AIC-iPSCs differentiated into functional beating AIC-iPSC-cardiomyocytes (CMs), which represents the cell-type of interest to study molecular, genetic and functional aspects of AIC.

1. Resource table

Unique stem cell line identifier	UMGi157-A
Alternative name(s) of stem cell line	AIC2.3
Institution	Clinic for Cardiology and Pneumology, University Medical Center Göttingen
Contact information of distributor	Katrin Streckfuss-Bömeke: katrin.streckfuss@med.uni-goettingen.de
Type of cell line	iPSC
Origin	Human
Additional origin info	Age: 49, Sex: male, Ethnicity if known: Caucasian
Cell Source	Skin fibroblasts isolated from skin biopsy
Clonality	Clonal
Method of reprogramming	Transduction with Sendai virus
Genetic Modification	No
Type of Modification	–
Associated disease	Arrhythmia-induced cardiomyopathy (AIC)
Gene/locus	–
Method of modification	–
Name of transgene or resistance	–
Inducible/constitutive system	–
Date archived/stock date	August 2019
Cell line repository/bank	–
Ethical approval	Ethical committee of University Medical Center Goettingen (Az −10/9/15)

2. Resource utility

Arrhythmia-induced cardiomyopathy (AIC) is caused by rapid and/or irregular ventricular rate. Pathomechanisms or predisposing genetics are not well understood to date (Sossalla and Vollmann, 2018). The generation of an iPSC-line from a patient diagnosed with AIC represents an excellent platform for genetic and physiological analysis to unravel the pathology underlying AIC (Fig. 1).

3. Resource details

AIC resembles a sub-form of dilated cardiomyopathy and is

* Corresponding author at: Clinic for Cardiology and Pneumology, University Medical Center Göttingen, Robert-Koch-Straße 40, 37075 Göttingen, Germany.
E-mail address: katrin.streckfuss@med.uni-goettingen.de (K. Streckfuss-Bömeke).
[1] These authors contributed equally.
[2] These authors contributed equally.

https://doi.org/10.1016/j.scr.2021.102263
Received 1 February 2021; Accepted 15 February 2021
Available online 20 February 2021

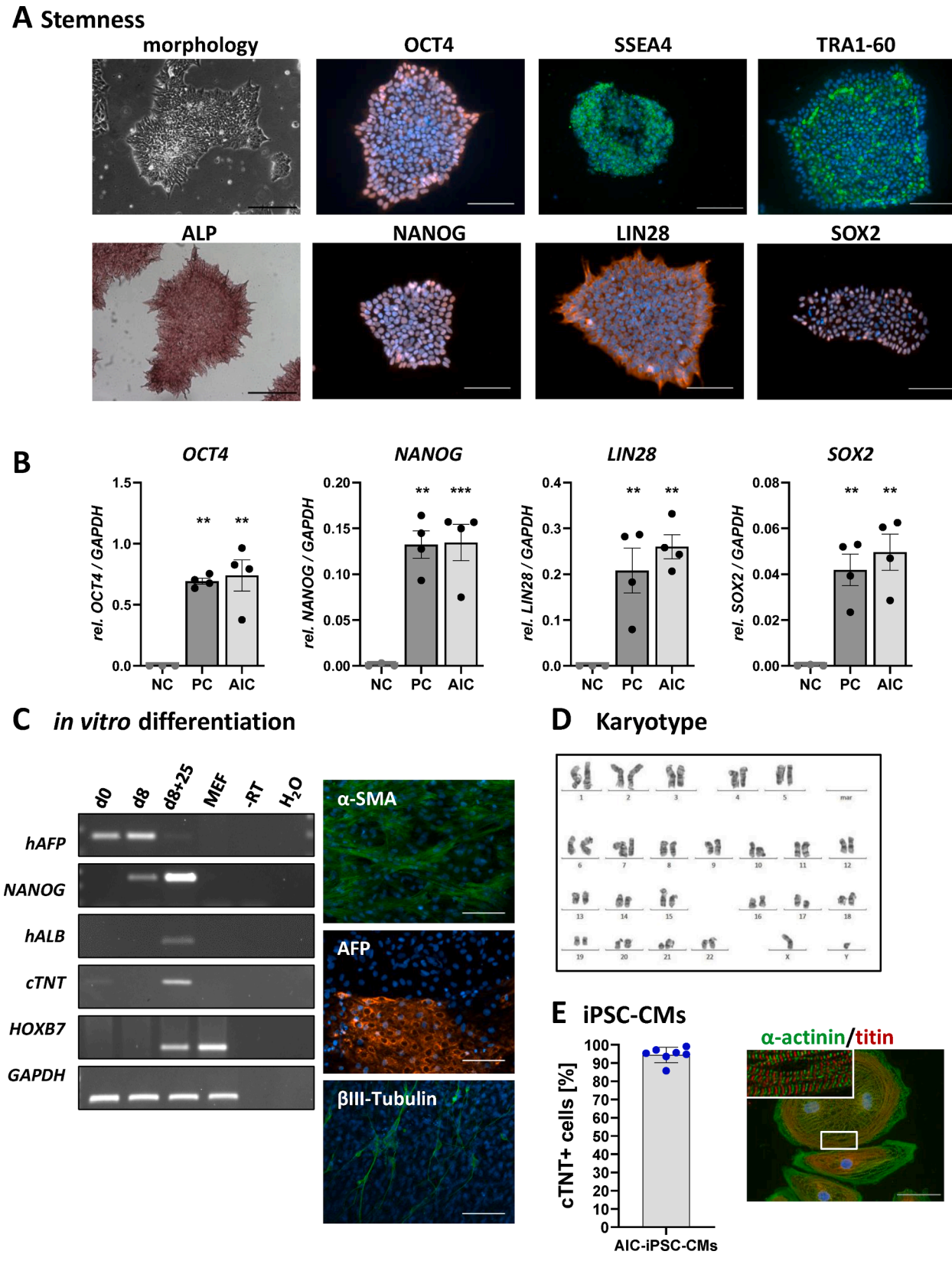

Fig. 1.

characterized by left-ventricular systolic dysfunction (LVSD), which is caused by rapid and/or irregular ventricular rate. The hallmark of this condition is partial or complete reversibility once arrhythmia control is achieved (Gopinathannair et al., 2015; Sossalla and Vollmann, 2018). Recent studies suggest that 56–88 % of patients with otherwise unexplained LVSD and concomitant tachyarrhythmia finally turn out to have a relevant component of AIC (Gopinathannair et al., 2015; Prabhu et al., 2017; Sossalla and Vollmann, 2018). Despite this high prevalence of

Table 1
Characterization and validation.

Classification	Test	Result	Data
Morphology	Photography	Round stem cell-like morphology	Fig. 1 panel A
Phenotype	Qualitative analysis	Positive immunofluorescence staining of pluripotency markers: OCT4, NANOG, SSEA4, LIN28, TRA1-60	Fig. 1 panel A
	Quantitative analysis (RT-qPCR)	Fold change for pluripotency genes (RT-qPCR) compared to NC: AIC-iPSCs *OCT4* = 1490 ± 412 *NANOG* = 119 ± 31 *LIN28* = 3657 ± 641 *SOX2* = 253 ± 69 The expression pattern of *OCT4, SOX2, NANOG*, and *LIN28* from AIC-iPSCs correlate with the expression pattern of a published iPSC-line (PC).	Fig. 1 panel B
Genotype	Karyotype (G-banding) and resolution	Karyotype: 46 XY, Resolution 300	Fig. 1 panel F
Identity	STR analysis	N/A STR: 16 gene loci were analyzed and matched	N/A submitted in archive with journal
Mutation analysis (IF APPLICABLE)	Sequencing Southern Blot OR WGS	– N/A	– N/A
Microbiology and virology	Mycoplasma	Negative mycoplasma testing by MycoAlert detection kit	Supplementary Table 1
Differentiation potential	Embryoid body formation	Germlayer marker expression on mRNA (RT-PCR) and protein level (immunofluorescence)	Fig. 1 panel E
Donor screening (OPTIONAL)	HIV 1 + 2 Hepatitis B, Hepatitis C	Donor material was negative for HIV, Hepatitis B, and Hepatitis C	data not shown
Genotype additional info (OPTIONAL)	Blood group genotyping	N/A	N/A
	HLA tissue typing	N/A	N/A

atrial tachyarrhythmias it remains unclear why only certain subjects of this patient cohort develop an AIC, suggesting that additional factors such as a genetic predisposition may play a role. Therefore, a patient diagnosed with AIC donated somatic material. This is a 49-year-old man with impaired left-ventricular ejection fraction (LVEF) and concomitant persistent atrial fibrillation. Coronary angiography and cardiac MRI ruled out other causes of LVSD. Upon persistent rhythm restoration, LVEF fully recovered and LVSD resolved within weeks, thereby confirming the diagnosis of AIC.

Induced pluripotent stem cells (iPSCs) were generated from skin fibroblasts of the AIC patient by transduction with Sendai virus (Fig. 1, Table 1). The AIC iPSC-line was authenticated by STR analysis and matched with the skin fibroblasts donated by the AIC patient. Generated AIC-iPSCs showed typical round colony-forming morphology and exhibited high activity of alkaline phosphatase (ALP) (Panel A, black scale bars: 200 μm). Furthermore, they expressed pluripotency-related proteins OCT4, NANOG, SSEA4, TRA1-60 and LIN28, which were visualized via immunofluorescence (Panel A, white scale bars: 100 μm). Furthermore, the AIC-iPSCs expressed pluripotency-related genes *OCT4*, *SOX2*, *LIN28* and *NANOG* similar to an already published control iPSC-line (Panel B, NC = negative control, PC = positive control). The differentiation capacity into cells of all three germ layers was assessed by embryoid body (EB) formation. The mRNA-expression of endodermal markers (α-feto-protein (*AFP)* and albumin (*ALB)*), mesodermal marker (troponin T *(cTNT)*) and ectodermal marker (homeobox B7 (*HOXB7)*) sequentially increased in EBs, while the expression of pluripotency-genes (*NANOG*) decreased (Panel C). In parallel, the AIC-iPSC-EBs showed positive signals for AFP, mesodermal α-smooth muscle actin (α-SMA), and ectodermal βIII-tubulin via immunofluorescence (Panel C, scale bars: 100 μm). G-banding karyotype analysis of the AIC-iPSCs demonstrated genomic integrity with a normal karyotype (Panel D). AIC-iPSCs were regularly tested negative for mycoplasma contamination (Supplementary Table 1). AIC affects the function of the heart ventricle, thus the efficiency to differentiate into iPSC-cardiomyocytes (CMs) was examined. Therefore, the AIC-iPSCs were differentiated into 90 days-old iPSC-CMs as described previously (Borchert et al., 2017). The AIC-iPSC-CMs showed autonomous beating and a high purity of cardiomyocytes demonstrated by flow cytometry of 85–99 % cTNT-positive cells for seven cardiac differentiation experiments (Panel E). Visualization of the sarcomere with antibodies against α-actinin (Z-disc) and titin-M8/M9 (M−line) demonstrated that AIC-iPSC-CMs have elongated cardiomyocyte morphology and formed a sarcomeric pattern (Panel E, scale bar: 50 μm). In conclusion, we successfully established and characterized an iPSC-line from a patient suffering from AIC. The AIC-iPSC-line exhibits full pluripotency properties with typical marker expression and high cardiac differentiation capacity. Thereof, the AIC-iPSC-line serves as an important human cell platform to study and elucidate the pathomechanisms of AIC.

4. Materials and methods

4.1. Reprogramming and cell culture

1x10^6 fibroblasts were incubated with 2.0 Sendai Reprogramming Kit (Thermo Fisher Scientific) with an MOI of 10:10:6 (KOS/hc-myc/hKLF4). The virus was mixed in fibroblast medium (DMEM (Thermo Fisher Scientific) with 10% FCS, 1x non-essential amino acids, 2 mM Glutamine, 50 μM β-Mercaptoethanol and 10 ng/ml bFGF), added to the cells and incubated for 24 h at 37 °C. On day 7 post transduction, the fibroblasts were passaged on a Geltrex®-coated 6-well plate in different ratios (1:4, 1:6, 1:8, 1:16, 1:20, 1:24) and medium was replaced with Essential 8 (E8) medium (Thermo Fisher Scientific). On day 12 post transduction, a suitable iPSC-colony was picked for expansion and characterization. The AIC-iPSCs were cultured in E8 medium (Thermo Fisher Scientific) and passaged when 80–90% confluency was reached as published previously (Hübscher et al., 2020). The cardiac differentiation was performed using sequential manipulation of Wnt-signaling as described earlier (Borchert et al., 2017).

4.2. In vitro differentiation

5.2x10^6 AIC2-iPSCs were mixed with 2.6x10^6 mouse embryonic fibroblasts and centrifuged at 250 g for 5 min. The cell-clump was then transferred to one 96-well plate well (U-bottom, Brand) in E8/TZV. The following day, medium was replaced with Iscove medium (Iscove basal medium (Thermo Fisher Scientific) with 20 % FCS, 1x non-essential amino acids, 450 μM methyl-thioglycolate) and changed every other day.

4.3. Mycoplasma detection

Routine testing for mycoplasma contamination was performed with MycoAlert detection Kit (Lonza) following the manufacturer's instructions. A ratio of 1.2 was set as a threshold.

4.4. RNA isolation and PCR analysis

Total RNA was isolated with the SV Total RNA Isolation System (Promega) following the manufacturer's instructions. RNA was treated

Table 2
Reagents details.

Antibodies used for immunocytochemistry/flow-cytometry			
	Antibody	Dilution	Company Cat # and RRID
Germlayer marker	rabbit anti-AFP	1:500	Dako, A0008 RRID AB_2650473
Germlayer marker	mouse anti-α-SMA	1:3000	Sigma, A2547RRID AB_476701
Germlayer marker	mouse anti-β-III-TUBULIN	1:2000	Covance, MMS-435P RRID AB_2313773
Pluripotency marker	goat anti-OCT4	1:40	R and D; AF1759 RRID AB_354975
Pluripotency marker	mouse anti-SOX2	1:200	R and D; MAB2018 RRID AB_358009
Pluripotency marker	goat anti-LIN28	1:300	R and D; AF3757 RRID AB_2234537
Pluripotency marker	goat anti-NANOG	1:50	R and D; AF1997 RRID AB_355097
Pluripotency marker	mouse anti-TRA1-60	1:200	Abcam, ab16288 RRID AB_778563
Pluripotency marker	mouse anti-SSEA4	1:200	Abcam, ab16287 RRID AB_778073
Sarcomeric marker	mouse anti-α-actinin	1:750	Sigma, A7811 RRID:AB_476766
Sarcomeric marker	rabbit anti-Titin-M8/M9	1:750	MyoMedix, TTN-9 RRID:AB_2734750
Secondary antibody	AF488 donkey anti-rabbit IgG	1:1000	Invitrogen, A31572 RRID AB_162543
Secondary antibody	AF555 donkey anti-goat IgG	1:1000	Invitrogen, A21432 RRID AB_141788
Secondary antibody	AF488 donkey anti-mouse IgG	1:1000	Invitrogen, A21202 RRID AB_141607
Secondary antibody	Cy3 goat anti-mouse IgG + IgM	1:300	Jackson Immuno, 115–165-068 RRID AB_2338686
Primers			
	Target	**Forward/Reverse primer (5′-3′)**	
Housekeeping gene (quantitative PCR)	*18 s*	ACCCGTTGAACCCCATTCGTGA/ GCCTCACTAAACCATCCAATCGG	
Housekeeping gene (semi-quantitative PCR)	*GAPDH*	AGAGGCAGGGATGATGTTCT/ TCTGCTGATGCCCCCATGTT	
Pluripotency marker (quantitative PCR)	*OCT4*	CCCCAGGGCCCCATTTTGGTACC/ ACCTCAGTTTGAATGCATGGGAGAGC	
Pluripotency marker (semi-quantitative and quantitative PCR)	*NANOG*	AGTCCCAAAGGCAAACAACCCACTTC/ ATCTGCTGGAGGCTGAGGTATTTCTGTCTC	
Pluripotency marker (quantitative PCR)	*SOX2*	GCTACAGCATGATGCAGGACCA/ TCTGCGAGCTGGTCATGGAGTT	
Pluripotency marker (quantitative PCR)	*LIN28*	AGCCATATGGTAGCCTCATGTCCGC/ TCAATTCTGTGCCTCCGGGAGCAGGGTAGG	
Germ layer marker (semi-quantitative PCR)	*AFP*	ACTCCAGTAAACCCTGGTGTTG/ GAAATCTGCAATGACAGCCTCA	
Germ layer marker (semi-quantitative PCR)	*ALB*	CCTTTGGCACAATGAAGTGGGTAACC/ CAGCAGTCAGCCATTTCACCATAGG	
Germ layer marker (semi-quantitative PCR)	*cTNT*	GACAGAGCGGAAAAGTGGGA/ TGAAGGAGGCCAGGCTCTAT	
Germ layer marker (semi-quantitative PCR)	*HOXB7*	GCCCTTTGAGCAGAACCTCTC/ CTTTTTCCACTTCATGCGCCG	

with 5 U DNase I (Zymo research) and cleaned with the clean and concentrator Kit (Zymo research). 200 ng of DNase-treated RNA was used for first-strand cDNA synthesis by employing the iScript cDNA synthesis Kit (Biorad). Semi-quantitative PCR was performed using GoTaq polymerase (Promega). Used primers are shown in Table 2. The PCR products were separated by electrophoresis on 2 % agarose gels. Quantitative PCR was performed using 1x iQ™ SYBR® Green Supermix (Biorad) and the iQ™5 real-time PCR detection system (Bio-Rad).

4.5. Immunofluorescence

AIC2-iPSCs and iPSC-CMs were fixated with 4 % Histofix solution (Sigma) for 15 min at room temperature and subsequently blocked in 1 % BSA overnight at 4 °C. The primary antibodies were incubated overnight at 4 °C. The fluorescently labelled secondary antibodies were added for 1 h at 37 °C (Table 2). Images were acquired with the Axiovert 200 fluorescence microscope (Zeiss) and the Axiovision software.

4.6. STR analysis

Genomic DNA was isolated using the QiAamp DNA mini Kit (Qiagen). STR analysis was performed by Eurofins Germany. For this, 16 gene loci were examined: AMEL, D8S1179, D21S11, D7S820, CSF1PO, D3S1358, D13S317, D16S539, D2S1338, D5S818, D19S433, D18S51, FGA, TH01, TPOX and vWA.

4.7. Karyotyping

85 % confluent iPSCs were incubated with 100 ng/μl demecolcine (Life technologies) for 16 h, trypsinized for 3 min and treated with 0.075 M KCl for 45 min at 37 °C. GTG-Banding (Gibco® Trypsin 1:250, ThermoFisher Scientific) of 8 metaphase spreads were analyzed and karyotyped using MetaClient 2.0.1. software (MetaSystems) on an Axio Imager Z2 microscope (Zeiss).

Declaration of Competing Interest

The authors declare that they have no known competing financial interests or personal relationships that could have appeared to influence the work reported in this paper.

Acknowledgments

The authors thank Johanna Heine, and Yvonne Metz (Clinic for Cardiology and Pneumology, UMG) and Ilona Eggert (Institute for Human Genetics, UMG) for superb technical support. This work was supported by the Fritz Thyssen Foundation [Az 10.19.2.026MN] to KSB and SS, and the German Heart Foundation/German Foundation of Heart Research [AZ. F/38/18] (to KSB). We acknowledge support by the Open Access Publication Funds of the Göttingen University.

Appendix A. Supplementary data

Supplementary data to this article can be found online at https://doi.org/10.1016/j.scr.2021.102263.

References

Borchert, T., Hübscher, D., Guessoum, C.I., Lam, T.-D.-D., Ghadri, J.R., Schellinger, I.N., Tiburcy, M., Liaw, N.Y., Li, Y., Haas, J., Sossalla, S., Huber, M.A., Cyganek, L., Jacobshagen, C., Dressel, R., Raaz, U., Nikolaev, V.O., Guan, K., Thiele, H., Meder, B., Wollnik, B., Zimmermann, W.-H., Lüscher, T.F., Hasenfuss, G., Templin, C., Streckfuss-Bömeke, K., 2017. Catecholamine-dependent β-adrenergic signaling in a pluripotent stem cell model of Takotsubo cardiomyopathy. J. Am. Coll. Cardiol. 70 (8), 975–991. https://doi.org/10.1016/j.jacc.2017.06.061.

Gopinathannair, R., Etheridge, S.P., Marchlinski, F.E., Spinale, F.G., Lakkireddy, D., Olshansky, B., 2015. Arrhythmia-induced cardiomyopathies: mechanisms,

recognition, and management. J. Am. Coll. Cardiol. 66 (15), 1714–1728. https://doi.org/10.1016/j.jacc.2015.08.038.

Hübscher, D., Rebs, S., Maurer, W., Ghadri, J.R., Dressel, R., Templin, C., Streckfuss-Bömeke, K., 2020. Generation of iPSC-lines from two independent Takotsubo syndrome patients with recurrent Takotsubo events. Stem Cell Res. 44, 101746. https://doi.org/10.1016/j.scr.2020.101746.

Prabhu, S., Taylor, A.J., Costello, B.T., Kaye, D.M., McLellan, A.J.A., Voskoboinik, A., Sugumar, H., Lockwood, S.M., Stokes, M.B., Pathik, B., Nalliah, C.J., Wong, G.R., Azzopardi, S.M., Gutman, S.J., Lee, G., Layland, J., Mariani, J.A., Ling, L.-H., Kalman, J.M., Kistler, P.M., 2017. Catheter ablation versus medical rate control in atrial fibrillation and systolic dysfunction: the CAMERA-MRI study. J. Am. Coll. Cardiol. 70 (16), 1949–1961. https://doi.org/10.1016/j.jacc.2017.08.041.

Sossalla, S., Vollmann, D., 2018. Arrhythmia-induced cardiomyopathy. Deutsches Arzteblatt Int. 115 (19), 335–341. https://doi.org/10.3238/arztebl.2018.0335.